Swarm Navigation in Lunar Caves: The First Proof-of-Concept Mission on Lanzarote

Siwei Zhang, Fabio Broghammer, Emanuel Staudinger, Robert Poehlmann,
Christian Gentner, Martin Schmidhammer, Armin Dammann
Institute of Communications and Navigation
German Aerospace Center (DLR)
Münchener Str. 20, 82234-Wessling, Germany
Siwei.Zhang@dlr.de

***Abstract*—Exploring lunar lava caves is currently under research spotlight. These caves could serve as ideal shelters for astronauts and instruments, protecting them from dramatic temperature variations and space radiation. However, so far, humans have only limited knowledge about these lunar caves. Robotic swarms are an emerging technology suitable for rapidly exploring large lunar caves. With the ability to optimize trajectories, the swarm can gather spatial-temporal information most efficiently. The nodes in the swarm form a self-organized radio network, providing multi-hop communications as well as precise time and position references without requiring additional infrastructure such as global navigation satellite systems (GNSSs) or base stations. In addition, the swarm can utilize either extra sensors or communication signals propagating through the network for environmental sensing. At the German Aerospace Center (DLR), we design compact and portable nodes with ultra-wide band (UWB) technology for decentralized timing, positioning, and environmental sensing. These nodes can be easily carried or deployed by robots and are thus suitable for proof-of-concept in space-analog missions. In this paper, we provide an overview of our UWB swarm navigation system following its development steps, namely designing mission concepts, establishing a self-organized network, conducting measurements, localizing the nodes, and performing radio-based environmental sensing. We also share insights from the first lunar-analog swarm cave navigation mission conducted in the lava cave *Cueva de los Naturalistas*, Lanzarote, in 2023, to demonstrate the navigation capabilities of our swarm.**

I. Introduction

Exploring lunar lava caves is currently under research spotlight [1]. These caves can be a hundred times larger than the ones on Earth due to the lower gravity on the Moon [2]. They could serve as ideal shelters protecting astronauts and instruments from dramatic temperature variation and space radiation. However, we currently have little knowledge about these lunar caves. Therefore, *in-situ* exploring those large lunar caves becomes the next holy-grail of space exploration. Robotic swarms are an emerging technology in which a massive number of robots collaborate to explore large areas. With the ability to optimize trajectories [3], swarms can efficiently gather and process spatial-temporal information from a macro and redundant perspective. This makes them well-suited for the rapid exploration of large lunar caves. For example, in the conceptual lava cave exploration mission depicted in Figure 1, a swarm of crawlers departs from the landing site, deploys sensor nodes, and collaboratively explores a lava cave on the Moon. The deployed nodes form a self-organized underground swarm network, providing multi-hop communications as well as time and position references without requiring additional infrastructure such as global navigation satellite systems (GNSSs) or base stations. Due to the high redundancy of the dense network, swarm communication and navigation remain highly reliable even in challenging environments with severe non-line-of-sight (NLOS) and multi-path propagation conditions, such as caves. Research has been intensively conducted in fields of self-organized networks [5], ultra-wide band (UWB) ranging [6] and network localization [7], [8]. However, there is little guidance on the system-level design of such a communication and navigation network for a real-world robotic swarm.

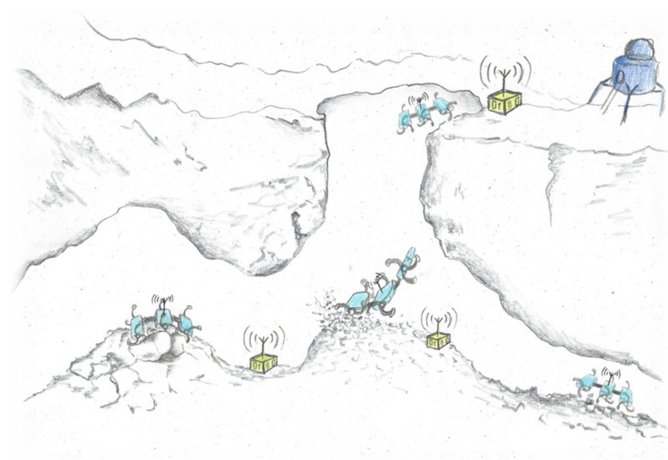

Fig. 1: A conceptual extraterrestrial surface and lava tube exploration mission [4].

At the Institute of Communications and Navigation of the German Aerospace Center (DLR), we have studied and developed radio-based swarm navigation technologies for more than a decade. As a latest evolution of our swarm system, we design compact, scalable and portable nodes with UWB technology, dubbed "UWB sensor eggs", for decentralized timing, position and environmental sensing [4], [9]. In this paper, we describe how to tailor our UWB sensor eggs for in-cave swarm navigation. We first propose a leapfrog navigation concept for caves, where no other navigation infrastructure is available. We then describe the self-organized time-division multiple access (SOTDMA) scheme for establishing an interference-free swarm network. Geometry measurements, such as three-way ranging (3WR) and three-way time difference of arrival (3W-TDoA), can be extracted from the UWB signals, effectively eliminating clock imperfections, including clock offsets and drifts. These measurements enable the localization of up to 20 active eggs and arbitrarily many passive eggs with an update rate of $5\,\mathrm{Hz}$. In addition, the massive date of the received raw signal samples from the mesh network reveals environmental information, such as the width, volume, or even the shape of the cave. This information is crucial for exploration decision-making and can further enhance swarm localization through simultaneous localization and mapping (SLAM) approaches.

As a highlight, we share insights on our swarm navigation experiment conducted in the lava cave *Cueva de los Naturalistas*, Lanzarote, 2023, which, to our best knowledge, is the first swarm navigation proof-of-concept targeting lunar caves. The experiment demonstrates the ability of our swarm to navigation and sense the environment in caves.

This paper provides a complete overview picture of our concepts, system design and first results from the analog mission, which sheds light on the usage of UWB for joint communication and navigation for a robotic swarm for future lunar cave exploration missions.

II. UWB Sensor Egg for Swarm Navigation

A. UWB Sensor Egg

We developed our "sensor eggs" swarm for localization and sensing applications based on Qorvo UWB modules. The ostrich-egg-sized sensor eggs have a fully self-organized and self-contained design. The egg shell is 3D-printed and airtight. Within an egg, as shown in Figure 2, we integrate a UWB transceiver (Qorvo DW1000), a Raspberry Pi 3 A+ microcomputer, a power-bank achieving a runtime of over $8\,\mathrm{h}$ and various replaceable environmental sensors. The UWB transceiver is driven by a low-cost quartz crystal oscillator with a drift of around 10 μs per second. This drift is negligible for establishing an SOTDMA structure, but not for propagation time-based measurements. Therefore, we model the measured time at an egg A as $t_\mathrm{A} \approx a_\mathrm{A}\ t + b_\mathrm{A}$, with its clock offset b_A and drift a_A. Schemes to handle these clock imperfections will be discussed in Section II-E. All components in an egg are off-the-shelf hardware, making the sensor eggs compact, cost-effective, and energy-efficient. As a result, they are easy to scale up and can be readily carried by a swarm of rovers or drones.

B. Swarm Network

Our swarm contains up to 20 active eggs, transmitting UWB signals every $200\,\mathrm{ms}$, and, in theory, an arbitrarily many passive eggs, only receiving UWB signals. The swarm forms a rigid mesh network with UWB signals, which keeps all the eggs localizable within the swarm. An exemplary swarm network is illustrated inFigure 3, with six active eggs (A, B, C, D, F, G) and a passive egg (E). Colored arrows shows the propagation directions of UWB signals which carry customized communication messages. For example, egg A transmits its message 1 $M_{\mathrm{A},1}$ at time $t_{\mathrm{A},1}$. The message includes the recorded transmission time $t^{\mathrm{A}}_{\mathrm{A},1}$, the recorded receiving time $t^{\mathrm{A}}_{\mathrm{B},0\to\mathrm{A}}$, $t^{\mathrm{A}}_{\mathrm{C},0\to\mathrm{A}}$ of messages 0 from egg B and C, respectively, the position estimate of A $\hat{\mathbf{p}_\mathrm{A}}$ and its covariance $\mathrm{cov}[\hat{\mathbf{p}_\mathrm{A}}]$. The transmission and receiving time tags are used for establishing an interference-free SOTDMA network in Section II-D and conducting measurements in Section II-E. The position estimate and its covariance are used for position estimation at neighboring eggs with, for example, distributed particle filters (DPFs).

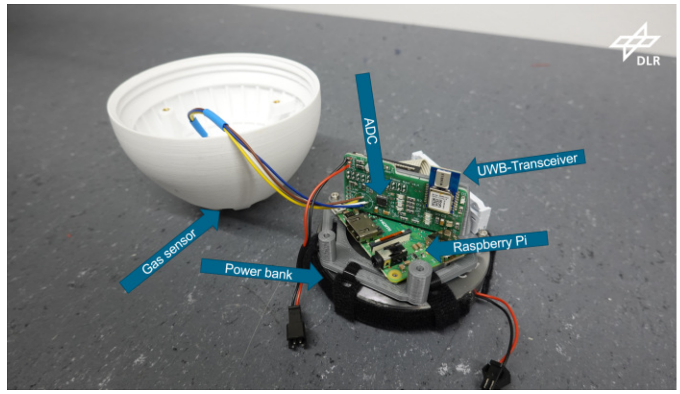

Fig. 2: An opened-up UWB sensor egg.

C. Leapfrog Navigation in Caves

We assume a lunar navigation infrastructure that only covers the entrance of the cave to be explored [10]. A large swarm network can exploit the concept of leapfrog navigation [11] to extend its exploration coverage deep into the cave step-by-step as illustrated in Figure 4. The eggs are grouped into two clusters. At the first step, the first cluster is deployed outside the cave, obtaining absolute position information from the lunar navigation infrastructure, while the second cluster is dropped into the cave being localized with the help of the first cluster. As the exploration continue, two clusters move in an alternating fashion, so that the stationary cluster provide localization assistance to the moving cluster. [11]

D. Self-Organized SOTDMA Network

A suitable media access control layer (MAC) protocol for swarms should adapt rapid topology and formation changes, be fully decentralized in order to avoid a single point of failure, and provide interference-free channel access. We design a SOTDMA protocol based on the DESYNC algorithm proposed in [5]. The basic concept is illustrated in Figure 5 with an exemplary three-egg network viewing at egg A. Each egg adjusts its transmission phase, i.e. the modulo transmission time

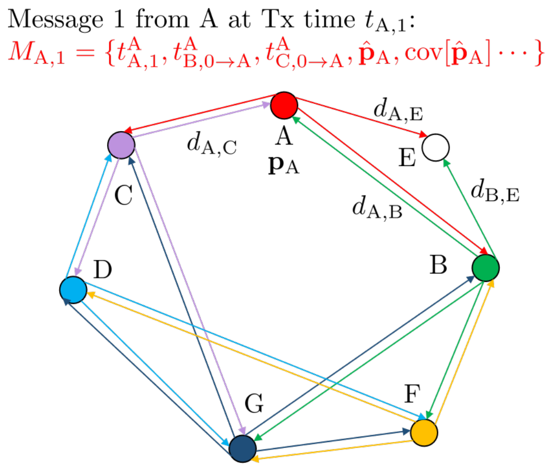

Fig. 3: An exemplary rigid swarm network with six active eggs and one passive egg.

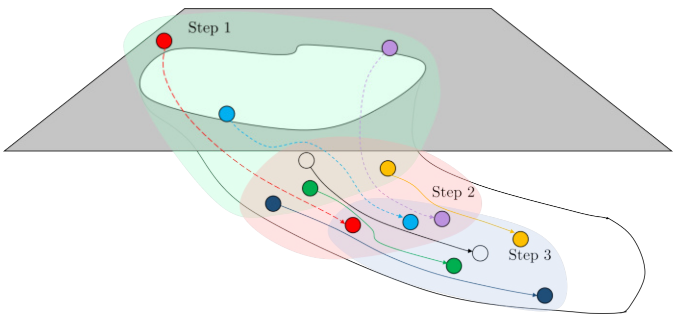

Fig. 4: Concept of leapfrog swarm navigation in a cave.

normalized to a time-division multiple access (TDMA) period, towards the middle point between its temporal neighbors. For example, the red egg A adjusts its transmission phase by observing the receiving time $t^{\mathrm{A}}_{\mathrm{C},0\to\mathrm{A}}$, $t^{\mathrm{A}}_{\mathrm{B},0\to\mathrm{A}}$ of its predecessor C and its successor B, respectively. The new transmission time for egg A is calculated as

$$t^{\mathrm{A}}_{\mathrm{A},1} = t^{\mathrm{A}}_{\mathrm{A},0} + T + \alpha\left(\left(t^{\mathrm{A}}_{\mathrm{B},0\to\mathrm{A}} - t^{\mathrm{A}}_{\mathrm{A},0}\right) - \left(t^{\mathrm{A}}_{\mathrm{A},0} - t^{\mathrm{A}}_{\mathrm{B},0\to\mathrm{A}}\right)\right), \tag{1}$$

where $0 \leq \alpha \leq 1$ is a discount factor to guarantee the convergence of a stable equally spaced SOTDMA structure [5]. DESYNC does not demand any central clock or pre-defined schedule. Therefore, it can support many eggs to join or leave the network. There are two problems with the original DESYNC, namely, hidden node and packet-loss, which may lead to instability of the SOTDMA structure. We solved these problems in [4] by adding receiving time, e.g. $t^{\mathrm{A}}_{\mathrm{B},0\to\mathrm{A}}$ and $t^{\mathrm{A}}_{\mathrm{C},0\to\mathrm{A}}$ into the communication messages as shown in Figure 3.

E. Measurements in Swarm Network

Obtaining propagation time-based measurements for localization is one of the key functionalities of the UWB signals, next to communications. We reuse the same messages as in Figure 3 for 3WR for active eggs, and 3W-TDoA for passive

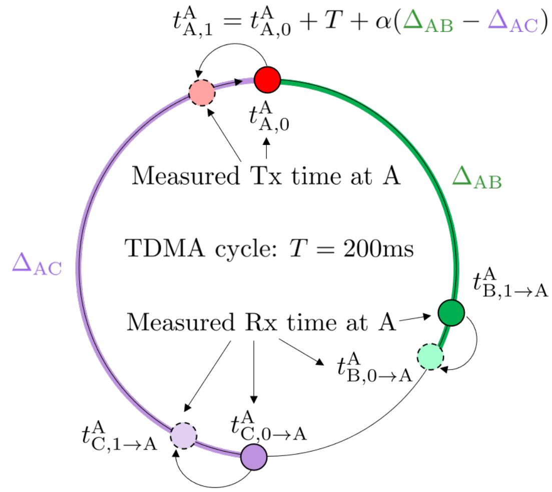

Fig. 5: SOTDMA scheme.

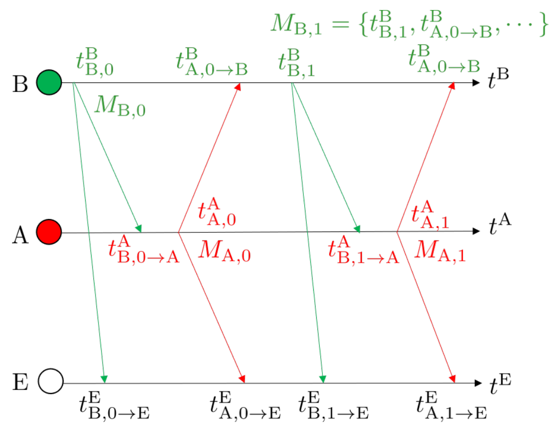

Fig. 6: Message exchange diagram for obtaining localization measurements

eggs. Both of these techniques eliminate the impacts of clock imperfections as discussed in [4]. In this paper, we only listed the final results for completeness. We assume an exemplary network with two active eggs A and B, and one passive egg E. The message exchange diagram for obtaining localization measurements is depicted in Figure 12.

1) Three-Way Ranging (TWR) between Active Eggs: The 3WR method can be applied to get the distance estimate between two active nodes, eliminating the impacts of unknown clock offsets and drifts. For example the distance between egg A and B can be estimated as

$$\begin{aligned}\hat{d}_{AB} =& c\frac{\left(t^{\mathrm{A}}_{\mathrm{B},1\to\mathrm{A}} - t^{\mathrm{A}}_{\mathrm{A},0}\right)\left(t^{\mathrm{B}}_{\mathrm{A},0\to\mathrm{B}} - t^{\mathrm{B}}_{\mathrm{B},0}\right)}{t^{\mathrm{A}}_{\mathrm{B},1\to\mathrm{A}} - t^{\mathrm{A}}_{\mathrm{B},0\to\mathrm{A}} + t^{\mathrm{B}}_{\mathrm{B},1} - t^{\mathrm{B}}_{\mathrm{B},0}} \\ &- c\frac{\left(t^{\mathrm{A}}_{\mathrm{A},0} - t^{\mathrm{A}}_{\mathrm{B},0\to\mathrm{A}}\right)\left(t^{\mathrm{B}}_{\mathrm{B},1} - t^{\mathrm{B}}_{\mathrm{A},0\to\mathrm{B}}\right)}{t^{\mathrm{A}}_{\mathrm{B},1\to\mathrm{A}} - t^{\mathrm{A}}_{\mathrm{B},0\to\mathrm{A}} + t^{\mathrm{B}}_{\mathrm{B},1} - t^{\mathrm{B}}_{\mathrm{B},0}}.\end{aligned} \tag{2}$$

The systematic remaining ranging error due to clock drifts is approximated as

$$\epsilon_{AB} \approx d_{AB}\left(\frac{a_A + a_B}{2} - 1\right), \tag{3}$$

which is negligible.

2) Time Difference of Arrival (TDoA) at Passive Eggs: One highlight of our system is to localize arbitrary many passive eggs by observing the 3W-TDoA from two active eggs, eliminating the clock imperfections from all eggs that are involved. The 3W-TDoA at a passive egg E with respect to active eggs A and B is defined as

$$d_{ABE} = d_{AE} - d_{BE}. \tag{4}$$

The 3W-TDoA can be obtained by

$$\begin{aligned}\hat{d}_{ABE} =& \frac{c}{2}\frac{\left(t^{\mathrm{E}}_{\mathrm{A},0\to\mathrm{E}} - t^{\mathrm{E}}_{\mathrm{B},0\to\mathrm{E}}\right)\left(t^{\mathrm{A}}_{\mathrm{B},1\to\mathrm{A}} - t^{\mathrm{A}}_{\mathrm{B},0\to\mathrm{A}}\right)}{t^{\mathrm{E}}_{\mathrm{B},1\to\mathrm{E}} - t^{\mathrm{E}}_{\mathrm{B},0\to\mathrm{E}}} \\ &- \frac{c}{2}\frac{\left(t^{\mathrm{E}}_{\mathrm{B},1\to\mathrm{E}} - t^{\mathrm{E}}_{\mathrm{A},0\to\mathrm{E}}\right)\left(t^{\mathrm{B}}_{\mathrm{B},1} - t^{\mathrm{B}}_{\mathrm{B},0}\right)}{t^{\mathrm{E}}_{\mathrm{B},1\to\mathrm{E}} - t^{\mathrm{E}}_{\mathrm{B},0\to\mathrm{E}}} \\ &+ \frac{c}{2}\left(\left(t^{\mathrm{B}}_{\mathrm{B},1} - t^{\mathrm{B}}_{\mathrm{A},0\to\mathrm{B}}\right) - \left(t^{\mathrm{A}}_{\mathrm{A},0} - t^{\mathrm{A}}_{\mathrm{B},0\to\mathrm{A}}\right)\right),\end{aligned} \tag{5}$$

where the systematic drift related error is approximated as

$$\epsilon_{ABE} \approx \left(\frac{a_A + a_B}{2} - 1\right)(d_{AE} - d_{BE}), \tag{6}$$

which is negligible.

With these obtained measurements, and the exchanged position estimates and covariances from neighboring eggs, each egg can estimate its own position with, for example, a DPF [9], [12].

F. Radio-Sensing

Cave environment is traditionally considered as radio-challenging due to the curvy path, and ubiquitous reflectors and scatters along the cave wall, which brings difficulty for localization. We extend the idea of channel SLAM [13], turning multi-paths into our friend for localization. Most channel SLAM algorithms, e.g. [13], [14], considers straight reflection surfaces, where surface mapping is reduced to estimating static virtual transmitters' positions. The straight surface assumption is valid in artificial environments like indoor and urban canyon. However, for natural unstructured environments like in caves, this assumption is no longer applicable. Our swarm mesh network with massive number of UWB links offers an opportunity to directly estimate the width, volume or even the shape of the curvy cave surfaces. Figure 7 illustrates one measurement snapshot, where line-of-sight (LOS) path and one reflected path can be estimated from the received signal, for example, with a super-resolution algorithm like space-alternating generalized expectation-maximization (SAGE). The LOS path corresponds to the distance between the transmitter (Tx) and the receiver (Rx). The reflected path defines an ellipsoid with Tx and Rx as the two focuses. The ellipsoid is tangential to the cave surface at an indefinite reflection points. With a single ellipsoid, only little information regarding the surface geometry can be extracted. However, with a swarm of N eggs, one may expect $O(N^2)$ number of ellipsoids per snapshot. When combining these massive number of ellipsoids, the surface geometry can become observable.

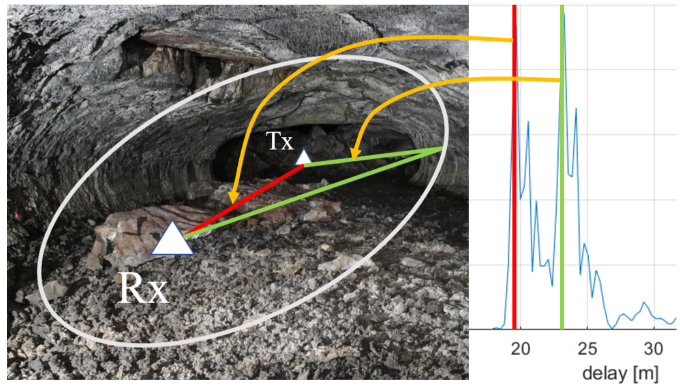

Fig. 7: One snapshot of reflection point sensing from the received signal propagated along the LOS path and one reflected path.

III. Experiment in a Lanzarote Lava Cave

In 2023, we conducted a swarm navigation experiment in a lava cave on Lanzarote named *Cueva de los Naturalistas*. The tube shaped cave is formed from lava flow during a volcanic eruption, which is similar to the cause of lava caves on the Moon. We expect that the inner surface of *Cueva de los Naturalistas* will have a similar radio-characteristic as a lunar lava cave. Therefore, it is a suitable testbed for lunar cave analog missions. The section of the cave for our experiment starts from a skylight and extends five meters underground for 200 meters. The average diameter of the section is around four meters. In total of 15 UWB sensor eggs were included in a six-step leapfrog navigation experiment. Fourteen eggs are stationary within every step. One egg (node 12) is mounted on a helmet and carried by a human. After each step, five stationary eggs were moved forward for the next step of leapfrog navigation. A leica total station is used for recording the ground-truth of all the eggs and for mapping the whole section of the cave into 3D point clouds. An impression of the experiment is shown in Figure 8. The overall scenario can be seen in Figure 9, including a top view and a side view of the cave and ground-truth of the egg deployment and trajectories. The steps are distinguished by different colors.

Massive data has been collected during the half-day experiment, including all the time tags of signal transmissions and receptions, 3WRs and 3W-TDoAs measurements, raw received signal samples, for every link in the network updated in 5 Hz. In this paper we focus on the sixth step, and discuss some preliminary results. The scenario of the sixth step can be seen in Figure 11, with one photo and the recorded egg trajectory and cave surface for an impression. We first look into the measurements obtained in step 6 from the moving egg 12 in Figure 12 together with the ground-truth distances. In Figure 12a we can see the 3WRs are in 10 cm accuracy in some sections, but are not available in other sections. It is due to the complex environment with NLOS propagation, but also due to the hardware imperfection, where sometimes the UWB transceiver is not able to transmit signals but only listen, for

Fig. 8: Swarm navigation experiments with 15 eggs and a leica total station for ground-truth.

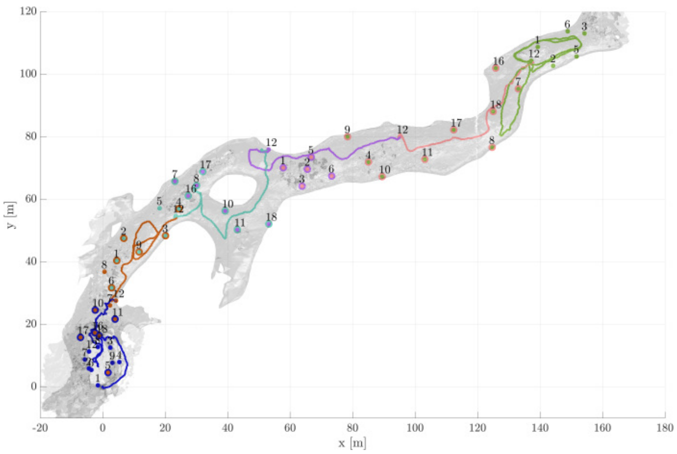

(a) Top view of the whole experiment scenario.

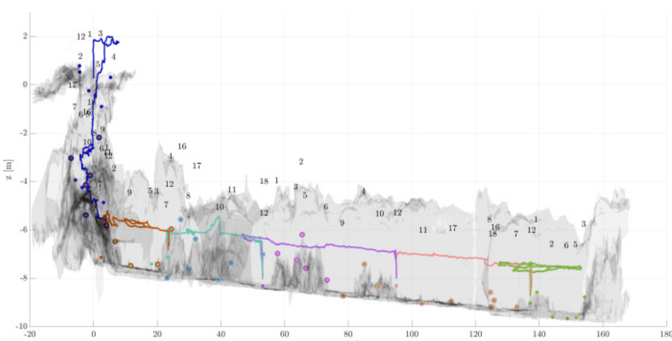

(b) Side view of the whole experiment scenario.

Fig. 9: Overview of the whole experiment scenario, recorded by the leica total station.

(a) A photo of step 6 scenario.

Fig. 10: s.

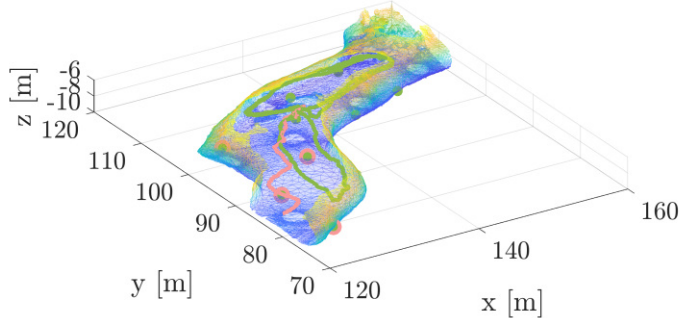

(a) Recorded egg trajectory and cave surface at step 6.

Fig. 11: Scenario of step 6.

example, from 18:01:00 till 18:01:30. Luckily, during this time period 3W-TDoA measurements can be continuously obtained, as shown in Figure 13, since it only requires the egg to listen. On average, we obtain 0.75 3WR and 3.3 3W-TDoA per UWB signal reception.

Then we investigate the localization performance of the moving node 12 in Figure 13. A particle filter is implemented for localization with only 3WR measurements on the left and with both 3WR and 3W-TDoA measurements on the right. One can see in both cases the particle filter provides accurate localization results and with both 3WR and 3W-TDoA measurements, it clearly outperforms the case of only considering 3WR measurements. This result is a strong evidence that our idea of having some active eggs and arbitrarily many passive eggs works.

Last but not least, we investigate the proposed radio-sensing approach in Figure 14. Egg 12 moves along the green trajectory with its estimate plotted in yellow. The received raw signal samples between the moving egg and two stationary eggs (3 and 16) are processed with SAGE algorithm. As an outcome, not only the LOS path but also the multi-paths are estimated. The multi-paths determine ellipsoids tangential to the cave surface if they are from signal reflections. As egg 12 moves, many ellipsoids are accumulated in Figure 14, which show a trace along the cave surface. It is only the first step towards a full swarm channel SLAM, but indicates that using the dense swarm network to directly sense unstructured environment is plausible.

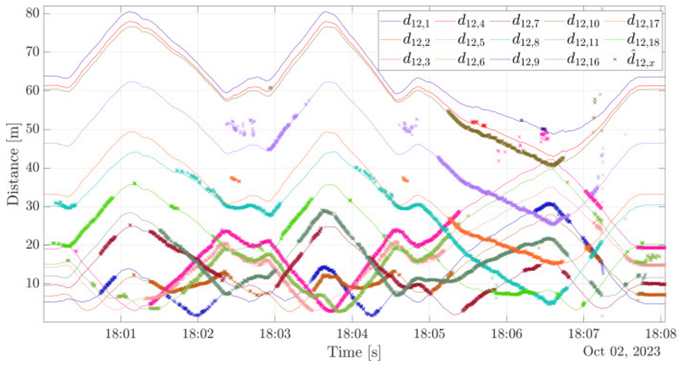

(a) 3WR measured at the moving node 12 vs. ground-truth distances.

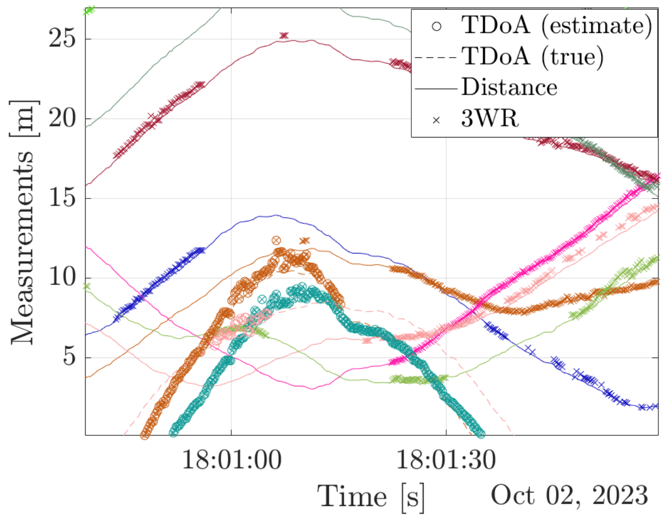

(b) 3WR and selected 3WR-TDoA measured at the moving node 12 vs. ground-truth distances.

Fig. 12: Measurements at the moving node 12 at step 6 vs. ground-truth distances.

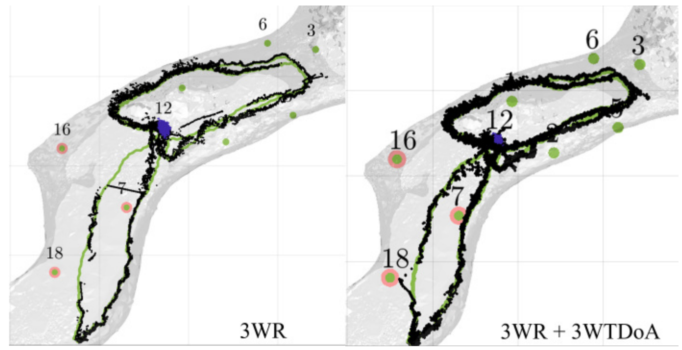

Fig. 13: Localization results with only 3WR measurements on the left and with both 3WR and 3W-TDoA measurements on the right.

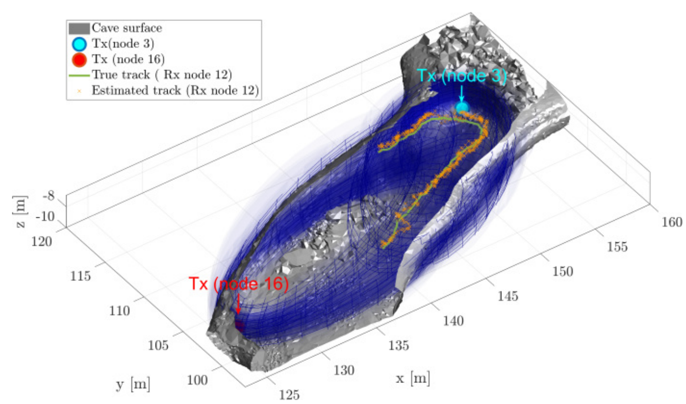

Fig. 14: Sensing the cave surface with a swarm.

IV. Conclusion

In this paper, we propose a swarm navigation approach fo lunar cave exploration missions. We depict an overview of our UWB sensor eggs which are suitable for such a mission. The system supports many active eggs and an arbitrary number of passive eggs. We conduct a large-scale swarm navigation experiment in a lava cave on Lanzarote, which we believe is the first lunar cave analog experiments of its kind. The preliminary results verify the overall system design, including self-organized network, leapfrog navigation concept, measurements for active and passive eggs with low cost clocks, localization, and radio-sensing in unstructured environment. It sheds light on future swarm exploration missions in lava caves on the Moon.

References

[1] L. Carrer, R. Pozzobon, F. Sauro *et al.*, "Radar evidence of an accessible cave conduit on the Moon below the mare tranquillitatis pit," *Nature Astronomy*, vol. 8, pp. 1119–1126, 2024. [Online]. Available: https://doi.org/10.1038/s41550-024-02302-y

[2] F. Sauro, R. Pozzobon, M. Massironi, P. De Berardinis, T. Santagata, and J. De Waele, "Lava tubes on Earth, Moon and Mars: A review on their size and morphology revealed by comparative planetology," *Earth-Science Reviews*, vol. 209, p. 103288, 2020. [Online]. Available: https://www.sciencedirect.com/science/article/pii/S0012825220303342

[3] S. Zhang, R. Pöhlmann, T. Wiedemann, A. Dammann, H. Wymeersch, and P. A. Hoeher, "Self-aware swarm navigation in autonomous exploration missions," *Proc. IEEE*, vol. 108, no. 7, pp. 1168–1195, 2020.

[4] S. Zhang, P. F. Ruz, F. Broghammer, E. Staudinger, C. Gentner, R. Poehlmann, A. Dammann, M. Schütt, and R. Lichtenheldt, "Self-organized UWB localization for robotic swarm – first results from an analogue mission on volcano Etna," in *2023 IEEE Aerospace Conference*, 2023, pp. 1–11.

[5] J. Degesys, I. Rose, A. Patel, and R. Nagpal, "DESYNC: Self-organizing desynchronization and TDMA on wireless sensor networks," in *2007 6th International Symposium on Information Processing in Sensor Networks*, 2007, pp. 11–20.

[6] D. Dardari, A. Conti, U. Ferner, A. Giorgetti, and M. Z. Win, "Ranging with ultrawide bandwidth signals in multipath environments," *Proc. IEEE*, vol. 97, no. 2, pp. 404–426, Feb. 2009.

[7] H. Wymeersch, J. Lien, and M. Win, "Cooperative localization in wireless networks," *Proc. IEEE*, vol. 97, no. 2, pp. 427–450, Feb. 2009.

[8] R. M. Buehrer, H. Wymeersch, and R. M. Vaghefi, "Collaborative sensor network localization: Algorithms and practical issues," *Proc. IEEE*, vol. 106, no. 6, pp. 1089–1114, Jun. 2018.

[9] F. Broghammer, T. Wiedemann, S. Zhang, A. Dammann, C. Gentner, and P. Djuric, "Self-organized sensor eggs for decentralized localization and sensing on Vulcano island – a glimpse into future space exploration with swarms," in *2024 27th International Conference on Information Fusion (FUSION)*, 2024, pp. 1–8.

[10] R. Pöhlmann, J. Gerhards, S. Zhang, E. Staudinger, and C. Becker, "Hybrid lunar satellite and cooperative surface navigation: A distributed

estimation perspective," in *Proceedings of the 2025 IEEE Aerospace Conference (AeroConf)*. Big Sky, MT, USA: IEEE, 2025.

[11] J. P. McIntire, F. C. Webber, D. K. Nguyen, Y. Li, S. Foong, K. Schafer, W. Y. Chue, K. Ang, E. T. Vinande, and M. M. Miller, "Leapfrogging: A technique for accurate long-distance ground navigation and positioning without GPS," *NAVIGATION*, vol. 65, no. 1, pp. 35–47, 2018. [Online]. Available: https://onlinelibrary.wiley.com/doi/abs/10.1002/navi.220

[12] S. Zhang, E. Staudinger, T. Jost, W. Wang, C. Gentner, A. Dammann, H. Wymeersch, and P. A. Hoeher, "Distributed direct localization suitable for dense networks," *IEEE Trans. Aerosp. Electron. Syst.*, vol. 56, no. 2, pp. 1209–1227, 2020.

[13] C. Gentner, T. Jost, W. Wang, S. Zhang, A. Dammann, and U.-C. Fiebig, "Multipath assisted positioning with simultaneous localization and mapping," *IEEE Transactions on Wireless Communications*, vol. 15, no. 9, pp. 6104–6117, 2016.

[14] E. Leitinger, F. Meyer, F. Hlawatsch, K. Witrisal, F. Tufvesson, and M. Z. Win, "A belief propagation algorithm for multipath-based SLAM," *IEEE Transactions on Wireless Communications*, vol. 18, no. 12, pp. 5613–5629, 2019.